

# Influence of the Snubbers and Matching Transformer on an Optimal Trajectory Controlled Resonant Transistor DC/DC Converter

Nikolay Dimitrov Bankov<sup>1</sup>, Aleksandar Stoyanov Vuchev<sup>1</sup>

**Abstract:** This work examines a series resonant DC/DC optimal trajectory controlled converter during operation above resonant frequency, taking into account the influence of the snubbers and matching transformer. We obtain expressions for the load characteristics, boundary curves between possible modes and limits of the soft commutation area. Computer simulation and experimental observation confirm the theoretical results.

**Keywords:** Series Resonant Converter, Optimal Trajectory Control.

## 1 Introduction

In recent years there have been extended discussions and comparisons of different methods of control of series DC/DC converters [1, 2]. One of these methods is optimal control on a selected converter operation trajectory. The advantages of this method over other control methods are reduction of the stresses on switches and reactive elements in the circuit and quick response in cases of important changes in the converter operating conditions without any effect on the stability of the entire circuit. On the other hand, it is known that operation above the resonant frequency results in better performance of the converters. This explains the considerable interest in series resonant converters operating at frequencies above their resonant frequency and with optimal trajectory control.

A number of publications [3 – 5] so far have presented theoretical analyses and have outlined the output and load characteristics of an optimal trajectory controlled resonant transistor DC/DC converter operating at frequencies higher than the resonant frequency. Usually the influence of the protection capacitors (snubbers) connected in parallel to the transistors is ignored and the matching transformer is assumed to be ideal with a transformation ratio of one unit. These

---

<sup>1</sup>Department of Electrical Engineering and Electronics, University of Food Technologies, 26 Maritza Blvd., 4002 Plovdiv, Bulgaria; E-mails: nikolay\_bankov@yahoo.com; avuchev@yahoo.com

analyses describe quite precisely the converter operation process, but they fail to clarify a very important event: the increase in load resistance disrupts the conditions for innate switching-on of the transistors at zero voltage (ZVS) and shuts the converter off. The analyses presented by [3] show that the higher the capacity of the snubbers, the more significant the error. Alternatively, the presence of a matching transformer can compensate for the influence of the snubbers and can also allow the converter to operate even in no-load mode.

The current article clarifies this event. A state plane analysis of an optimal trajectory controlled resonant transistor DC/DC converter is done, taking into consideration the influence of the snubbers and the matching transformer. The possible operating modes of the converter are examined and its output characteristics in relative units are plotted. Both the boundary lines between the separate operating modes of the converter in the output characteristics plane and the innate commutation area of the transistors are shown. A computer simulation and an experimental prototype confirmed the analytical results.

## 2 Operating Modes of the Converter

Fig. 1 shows the electrical circuit of the examined converter. It consists of an inverter (transistors  $Q_1-Q_4$  with freewheeling diodes  $D_1-D_4$ ), a resonant circuit ( $L$  and  $C$ ), a matching transformer ( $Tr$ ), an uncontrolled rectifier ( $D_5-D_8$ ), a filter capacitor ( $C_{F2}$ ), and a load resistor ( $R_0$ ). The snubbers ( $C_1-C_4$ ) are connected in parallel to the transistors. For the purpose of the analysis, they are substituted by one equivalent capacitor with capacity  $C_S = C_1-C_4$ , which is connected to the inverter output.

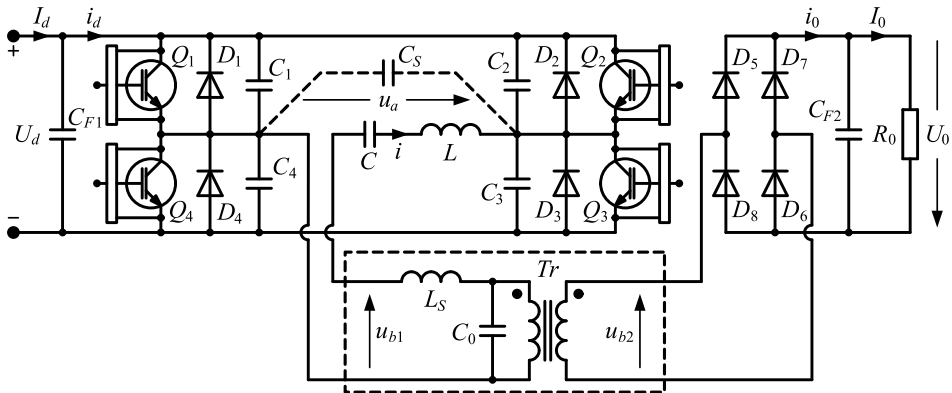


Fig. 1 – Circuit of the converter.

The matching transformer  $Tr$  is presented by means of its simplified equivalent circuit, which consists of the total leakage inductance  $L_S$  and the self-capacity of coils  $C_0$ , related to the primary coil, and a single ideal transformer

with transformation ratio  $k$  [6, 7]. The leakage inductance  $L_S$  is connected in series with the resonant tank inductance  $L$  and it can be viewed as part of the inductance  $L$ . The self-capacity  $C_0$  indicates both the capacity between the coils and the capacity between the windings and the separate layers of each coil of the matching transformer.

With more significant change in the load and the operating frequency, three different converter operating modes can be observed.

It is characteristic for the first mode that the commutations in the rectifier occur entirely in the intervals for conduction of the transistors in the inverter. This mode is the main operation mode of the converter. It is observed at comparatively small values of the load resistor  $R_0$ .

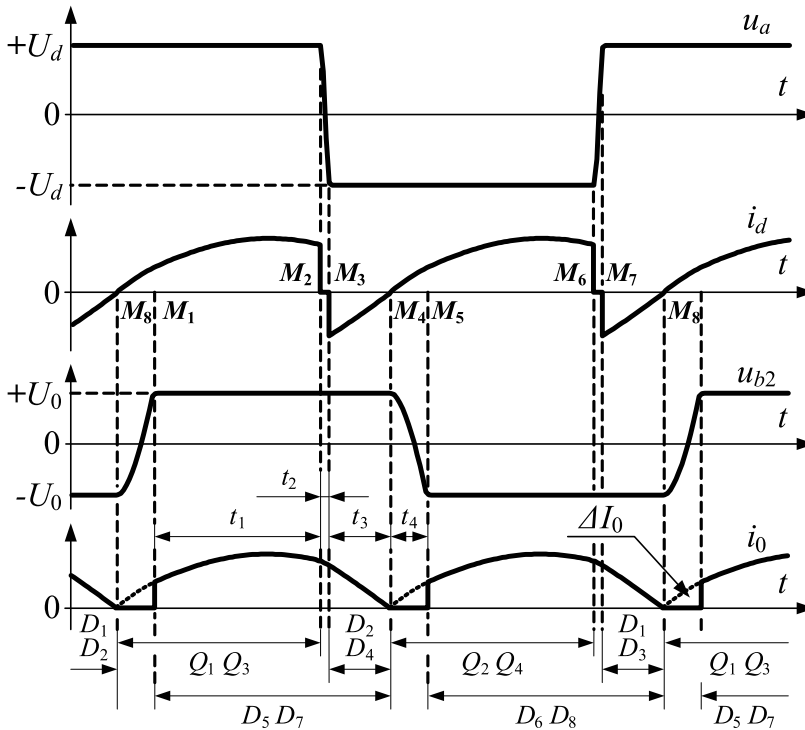


**Fig. 2** – Waveforms of the converter voltages and currents at the main operating mode.

Under the second operating mode the rectifier commutation ends during the inverter commutation; that is, the rectifier diodes start conducting when both the transistors and the freewheeling diodes of the inverter are turned off. This operating mode is *medial* and it takes place in the narrow zone of change in the load resistor value, but not very close to no-load.

The third case occurs in operating modes which are close to no-load. The rectifier commutations now end after those of the inverter; that is, the rectifier diodes start conducting after the respective freewheeling diodes of the inverter have been switched on. This operating mode is *conterminal* to no-load mode.

The *main* operating mode of the converter is illustrated by means of both the waveforms in Fig. 2 and the presented point trajectory in a state plane ( $x = U'_c; y = I'$ ) [8], which is shown in Fig. 3.

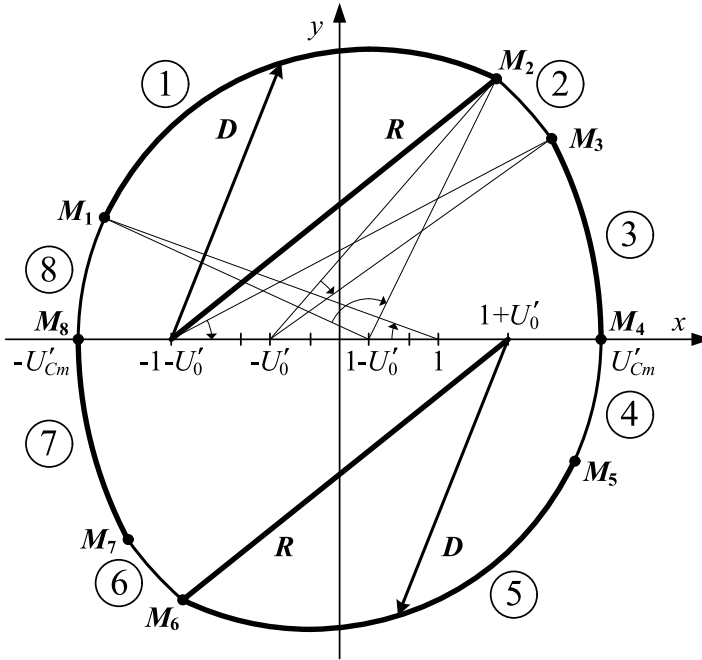


Fig. 3 – Presentation point trajectory in the main operating mode.

The method of optimal control uses a selected operation trajectory as a control law. The control parameter characterizing the individual operation trajectory is distance  $R$ , measured between the coordinates' centre  $(-1-U'_0; 0)$  and point  $M_2$  on the presentation point trajectory.

In the first half-cycle, distance  $D$  to the trajectory is monitored, measured from the coordinates' centre  $(-1-U'_0; 0)$ . If this distance is shorter than distance  $R$ , which is set by the controlling system, then transistors  $Q_1/Q_3$  are switched on (arc  $M_1M_2$ ). At point  $M_2$  distance  $D$  becomes equal to  $R$ , causing  $Q_1/Q_3$  to switch off, and the re-charging of  $C_S$  starts up (arc  $M_2M_3$ ). In p. $M_3$  diodes  $D_2/D_4$  are switched on (arc  $M_3M_4$ ). In p. $M_4$  the resonant current changes its direction, the diodes are switched off, and the re-charging of  $C_0$  starts up

(arc  $M_4M_5$ ). After this transistors  $Q_2/Q_4$  are switched on (arc  $M_5M_6$ ). Distance  $D$  is monitored again, measuring from the coordinate centre  $(1+U'_0;0)$ . The processes in the circuit then repeat.

### 3 Analysis of the Converter

For the purposes of this analysis, it is assumed that all elements of this circuit (except for the matching transformer) are ideal, and the ripples of the input voltage  $U_d$  and the output voltage  $U_0$  are ignored.

In order to obtain general results, it is necessary to normalize all quantities characterizing the converter's state. The following quantity symbols are used in relative units:

$$x = U'_C = u_c / U_d \text{ - voltage across the capacitor } C,$$

$$y = I' = \frac{i}{U_d / \rho_0} \text{ - current through the inductor } L,$$

$$U'_0 = kU_0 / U_d \text{ - output voltage,}$$

$$I'_0 = \frac{I_0 / k}{U_d / \rho_0} \text{ - output current,}$$

$$U'_{Cm} = U_{Cm} / U_d \text{ - peak voltage across the capacitor } C,$$

$$v = \omega / \omega_0 \text{ - frequency distraction of the resonant circuit,}$$

where  $\omega$  is the operating frequency, and  $\omega_0 = 1/\sqrt{LC}$  and  $Z_0 = \sqrt{L/C}$  are the resonant frequency and the characteristic impedance of the resonant tank circuit, respectively.

The following designations are also made:

$$a_1 = C_S / C, \quad a_2 = C_0 / C,$$

$$n_1 = \sqrt{(a_1 + 1)/a_1}, \quad n_2 = \sqrt{(a_2 + 1)/a_2}, \quad n_3 = \sqrt{1 + 1/a_1 + 1/a_2}.$$

Regarding the influence of both the snubbers and the matching transformer, the average value of the output current  $I'_0$  is obtained on the basis of the known expressions taken from [9] and [10]:

$$I'_0 = 2vU'_{Cm} / \pi - \Delta I'_0 = 2v(U'_{Cm} - a_2 U'_0) / \pi. \quad (1)$$

On the other hand, the dependence is known:

$$\frac{\pi}{v} = \omega_0 (t_1 + t_2 + t_3 + t_4), \quad (2)$$

where  $t_1, t_2, t_3, t_4$  represent the times of the four intervals in the *main* (Fig. 2) or the *conterminal* operating mode of the converter for one half-cycle.

For the *main* operating mode, the times  $t_1, t_2, t_3, t_4$  are determined as follows:

$$t_1 = \begin{cases} \frac{1}{\omega_0} \left( \operatorname{arctg} \frac{y_2}{-x_2 + 1 - U'_0} - \operatorname{arctg} \frac{y_1}{-x_1 + 1 - U'_0} \right), & x_1, x_2 \leq 1 - U'_0, \\ \frac{1}{\omega_0} \left( \pi - \operatorname{arctg} \frac{y_2}{x_2 - 1 + U'_0} - \operatorname{arctg} \frac{y_1}{-x_1 + 1 - U'_0} \right), & x_1 \leq 1 - U'_0 \leq x_2, \\ \frac{1}{\omega_0} \left( \operatorname{arctg} \frac{y_2}{-x_2 + 1 - U'_0} + \operatorname{arctg} \frac{y_1}{x_1 - 1 + U'_0} \right), & x_1, x_2 \geq 1 - U'_0, \end{cases} \quad (3)$$

$$t_2 = \begin{cases} \frac{1}{n_1 \omega_0} \left( \operatorname{arctg} \frac{n_1 y_2}{x_2 - 1 + U'_0} - \operatorname{arctg} \frac{n_1 y_3}{x_3 + 1 + U'_0} \right), & x_2 \geq 1 - U'_0, \\ \frac{1}{n_1 \omega_0} \left( \pi - \operatorname{arctg} \frac{n_1 y_2}{-x_2 + 1 - U'_0} - \operatorname{arctg} \frac{n_1 y_3}{x_3 + 1 + U'_0} \right), & x_2 \leq 1 - U'_0, \end{cases} \quad (4)$$

$$t_3 = \frac{1}{\omega_0} \operatorname{arctg} \frac{y_3}{x_3 + 1 + U'_0}, \quad (5)$$

$$t_4 = \begin{cases} t_4 = \frac{1}{n_2 \omega_0} \left( \operatorname{arctg} \frac{n_2 y_1}{-x_1 + 1 - U'_0} \right), & x_1 \leq 1 - U'_0, \\ t_4 = \frac{1}{n_2 \omega_0} \left( \pi - \operatorname{arctg} \frac{n_2 y_1}{x_1 - 1 + U'_0} \right), & x_1 \geq 1 - U'_0. \end{cases} \quad (6)$$

In the expressions above, for each of the intervals the normalized initial values of the voltage across the capacitor  $C$  and the current through the inductor  $L$  are signified by means of  $x_1-x_4$  and  $y_1-y_4$  respectively:

$$x_1 = -U'_{Cm} + 2a_2 U'_0, \quad (7)$$

$$y_1 = \sqrt{4a_2 U'_0 (U'_{Cm} - a_2 U'_0 + 1)}, \quad (8)$$

$$x_2 = U'_0 U'_{Cm} - a_2 U'^2_0 - a_1, \quad (9)$$

$$y_2 = \sqrt{\left( \begin{aligned} &(-U'_{Cm} + 2a_2 U'_0 - U'_0 U'_{Cm} + a_2 U'^2_0 + a_1) \cdot \\ &\cdot (-U'_{Cm} + 2a_2 U'_0 + U'_0 U'_{Cm} - a_2 U'^2_0 - a_1 + 2U'_0 - 2) + \\ &+ 4a_2 U'_0 (U'_{Cm} - a_2 U'_0 + 1) \end{aligned} \right)}, \quad (10)$$

$$x_3 = U'_0 U'_{Cm} - a_2 U'^2_0 + a_1, \quad (11)$$

$$y_3 = \sqrt{(U'_{Cm} - U'_0 U'_{Cm} + a_2 U'^2_0 - a_1) \cdot (U'_{Cm} + U'_0 U'_{Cm} - a_2 U'^2_0 + a_1 + 2U'_0 + 2)}, \quad (12)$$

$$x_4 = U'_{Cm}, \quad (13)$$

$$y_4 = 0. \quad (14)$$

In the *conterminal* operating mode, for the times  $t_1, t_2, t_3, t_4$  the following expressions are obtained:

$$t_1 = \begin{cases} \frac{1}{n_2\omega_0} \left( \operatorname{arctg} \frac{y_2^0}{1-x_2^0} \right), & x_2^0 \leq 1, \\ \frac{1}{n_2\omega_0} \left( \pi - \operatorname{arctg} \frac{y_2^0}{x_2^0-1} \right), & x_2^0 \geq 1, \end{cases} \quad (15)$$

$$t_2 = \begin{cases} \frac{1}{n_3\omega_0} \left( \pi - \operatorname{arctg} \frac{n_3 y_2^0}{n_2(1-x_2^0)} - \operatorname{arctg} \frac{n_3 y_3^0}{n_2(1+x_3^0)} \right), & x_2^0 \leq 1, \\ t_2 = \frac{1}{n_3\omega_0} \left( \operatorname{arctg} \frac{n_3 y_2^0}{n_2(x_2^0-1)} - \operatorname{arctg} \frac{n_3 y_3^0}{n_2(1+x_3^0)} \right), & x_2^0 \geq 1, \end{cases} \quad (16)$$

$$t_3 = \frac{1}{n_2\omega_0} \left( \operatorname{arctg} \frac{y_3^0}{1+x_3^0} - \operatorname{arctg} \frac{y_4^0}{1+x_4^0} \right), \quad (17)$$

$$t_4 = \frac{1}{\omega_0} \left( \operatorname{arctg} \frac{y_4}{x_4 + 1 + U'_0} \right). \quad (18)$$

In that case, for each of the intervals the normalized initial values of the voltage across the capacitor  $C$  and the current through the inductor  $L$  are signified by means of  $x_1^0, x_2^0, x_3^0, x_4^0$  and  $y_1^0, y_2^0, y_3^0, y_4^0$  respectively:

$$x_1^0 = -U'_{Cm} - U'_0, \quad (19)$$

$$y_1^0 = 0, \quad (20)$$

$$x_2^0 = \frac{(U'_{Cm} - a_2 U'_0)(1 + U'_0 + a_2 U'_0)}{a_2} - a_1 n_2^2, \quad (21)$$

$$y_2^0 = \sqrt{(U'_{Cm} + 1 + U'_0)^2 - (1 - x_2^0)^2}, \quad (22)$$

$$x_3^0 = \frac{(U'_{Cm} - a_2 U'_0)(1 + U'_0 + a_2 U'_0)}{a_2} + a_1 n_2^2, \quad (23)$$

$$y_3^0 = \sqrt{(x_2^0)^2 + (y_2^0)^2 - (x_3^0)^2}, \quad (24)$$

$$x_4^0 = -U'_{Cm} + U'_0(1 + 2a_2), \quad (25)$$

$$y_4^0 = 2\sqrt{(a_2 U'_0 + 1 + U'_0)(a_2 U'_0 - U'_{Cm})}. \quad (26)$$

In the *medial* operating mode, the sinusoidal quantities of the different operating intervals have four different angular frequencies. Therefore, in that case, the analysis is much more complicated and has not been carried out by the authors.

#### 4 Output Characteristics and Boundary Curves

In the main operating mode the controlling parameter  $R$  is defined by the coordinates of point  $M_2$  from the trajectory shown in Fig. 3:

$$R = \sqrt{(1 + U'_0 + x_2)^2 + y_2^2}. \quad (27)$$

In this case, by means of (9) and (10),  $U'_{Cm}$  is defined depending on the distance  $R$ , output voltage  $U'_0$ , and capacitor ratio  $a_1$ :

$$U'_{Cm} = -1 - U'_0 + \sqrt{R^2 + 4a_1}. \quad (28)$$

Applying the above expression for (7–13) eliminates  $U'_{Cm}$ . After that, through consecutive substitution of (7–13) in (3–6) and (3–6) in (2), the following dependency type is acquired:  $U'_0 = f(I'_0, R, a_1, a_2)$ . Solving this dependency makes it possible to outline the output characteristics in relative units under optimal trajectory control of the converter for the *main* operating mode. Such characteristics are shown in Fig. 4 for  $R = 1.4; 2.2; 3.0; 4.0; 5.0; 6.0$  and  $a_1 = 0.1; a_2 = 0.2$ .

In the *conterminal* operating mode, the distance  $R$  can be obtained again by means of expression (27), where:

$$x_2 = x_2^0/n_2^2, \quad y_2 = y_2^0/n_2. \quad (29)$$

After substitution of the (29) to (27),  $U'_{Cm}$  can be defined depending on the distance  $R$ , output voltage  $U'_0$ , and capacitor ratios  $a_1$  and  $a_2$ .

The expression for  $U'_{Cm}$  substitutes in (19–26). Then, substituting consecutively (19–26) in (15–18) and (15–18) in (2), the following dependency is acquired:  $U'_0 = f(I'_0, R, a_1, a_2)$ . Solving this dependency makes it possible to outline the output characteristics in relative units under optimal trajectory control of the converter for the *conterminal* operating mode. Such characteristics are shown in Fig. 4 for  $R = 2.2; 3$  and  $a_1 = 0.1; a_2 = 0.2$ .

Comparison of these characteristics with the characteristics known from [5] shows the total effect of the snubbers and the self-capacity of the matching transformer. It is evident that the output characteristics become more vertical



and the converter can be viewed more as a power supply unit, which will be reliable during work and at short-circuit incidence. In addition, an area of operation is outlined where  $U'_0 > 1$ .

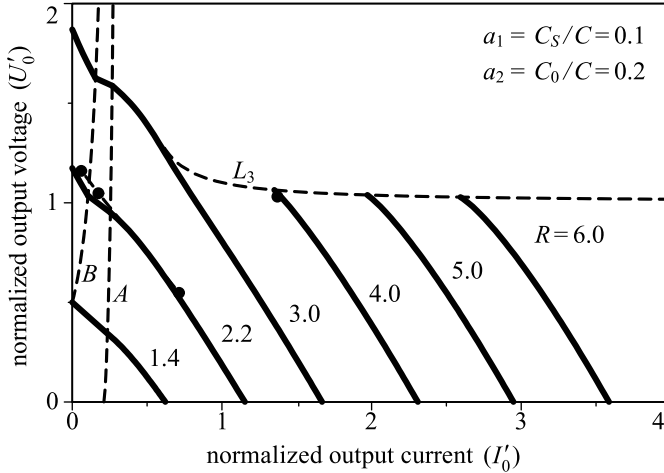


Fig. 4 – Output characteristics of the converter.

With the purpose of providing natural switching-on of the transistors at zero voltage (ZVS), the inverter commutations (stages 2 and 6) should always end before the current through the resonant tank circuit resets back to zero. This can be guaranteed only under the following condition:

$$x_3 \leq U'_{Cm} . \tag{30}$$

If condition (30) is not maintained, switching off one transistor pair will not result in switching on the other transistor pair at zero voltage, and then the converter will stop working.

It is a fact that the converter can work in the *main* and *conterminal* operating modes if the following conditions are met, respectively:

$$x_1 \leq x_2 ; \quad x_4^0 \geq x_3^0 . \tag{31}$$

Inequalities (30) and (31) help to draw (Fig. 7) the boundary of natural commutation, curve  $L_3$ , as well as the boundary curves  $A$  and  $B$  between the *main* and the *medial* mode and between the *medial* and the *conterminal* mode respectively on the output characteristics plane. It can be seen that the main operating mode area is limited between the boundary curves  $A$  and  $L_3$ . The higher the capacity of the snubbers and the self-capacity of the coordinate transformer coils, the smaller this area appears to be. However, increasing the snubbers capacity leads to a decrease in the commutation losses within the transistors and to limitation of the electromagnetic disturbances of the converter.

The *conterminal* operating mode area is limited by both the axis of ordinates and the boundary curve  $B$ . It can be seen that the converter stays absolutely fit for work at high-Ohm loads, including in no-load mode. This is due mainly to the capacitor  $C_0$ . With the increase in its capacity (increase in  $a_2$ ) the area of the boundary operation mode can also be increased.

Analysis in the *medial* operating mode has not been realized, but in the plane of the output characteristics its area is defined by the boundary curves  $A$  and  $B$ , standing respectively for the *main* and the *conterminal* operating modes. Taking into account the monotonous character of the output characteristics of the other two modes, the reviewed operating mode can only be outlined with the help of linear interpolation. This is shown in Fig. 4 for  $R = 1.4; 2.2$  and  $3.0$ . The area of this operating mode increases in proportion to the increase in the capacity of the snubbers  $C_S$  and the reduction in the self-capacity  $C_0$  of the coordinate transformer.

## 5 Simulation and Experimental Results

With the help of a known method from [9], a resonant transistor DC/DC converter operating at frequencies higher than the resonant frequency is designed with the following output parameters:  $P = 2$  kW;  $f = 50$  kHz;  $U_d = 250$  V. The values of the resonant circuit elements are as follows:  $C = 65.276$  nF,  $L = 102.639$   $\mu$ H. With the aim of proving the acquired theoretical results, coefficients  $a_1 = 0.1$ ;  $a_2 = 0.2$  and  $k = 10$  are chosen, corresponding to values  $C_1-C_4 = 6.5276$  nF and  $C_0 = 13.055$  nF, respectively.

The computer simulation model with OrCAD PSpice is by [11]. The matching transformer leakage inductance  $L_S$  is ignored. Computer simulation at  $R = 2.2$  and load resistance of  $R_0 = 3, 23,$  and  $70$  k $\Omega$  as well as at  $R = 4.0$  and  $R_0 = 3$  k $\Omega$  is performed. The acquired points from the converter output characteristics are shown in Fig. 4. A good match between the theoretical results and the results from the computer simulation can be observed, and this confirms the accuracy of the acquired results. The differences between the results are mainly due to the losses during the turned-on state of the semiconductor switches.

Figs. 5, 6, and 7 show waveforms of characteristic quantities illustrating respectively the main, medial, and *conterminal* operation activity of the converter. These are the current through the resonant circuit,  $I(L)$ , the output voltage from the inverter,  $V(A)$ , and the input voltage to the matching transformer,  $V(B1)$ . The simulations are performed at  $R = 2.2$  and  $R_0 = 3, 23,$  and  $70$  k $\Omega$ , and they correspond to the output characteristics points of the converter from Fig. 4. Figs. 5 and 7 show points  $M_1-M_8$ , illustrating the moments of commutation in the converter.

Influence of the Snubbers and Matching Transformer on an Optimal Trajectory...

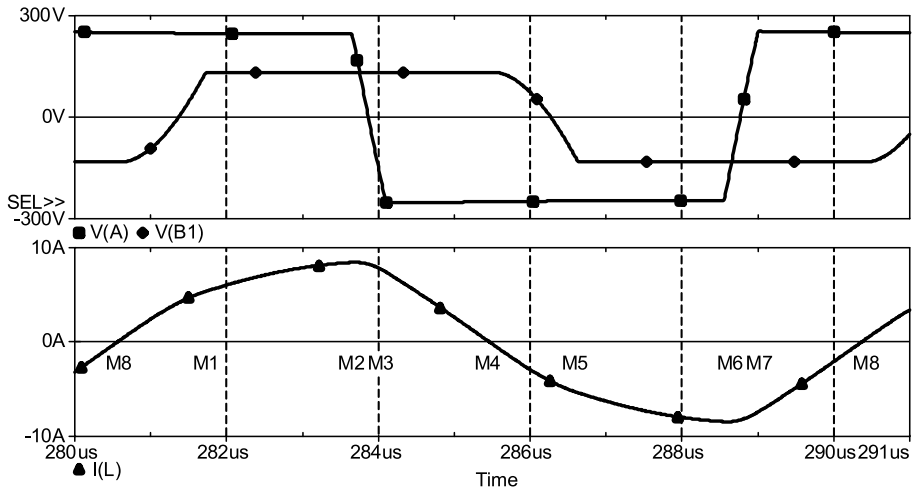


Fig. 5 – Simulation results in the main operating mode ( $R = 2.2$  and  $R_0 = 3$  k $\Omega$ ).

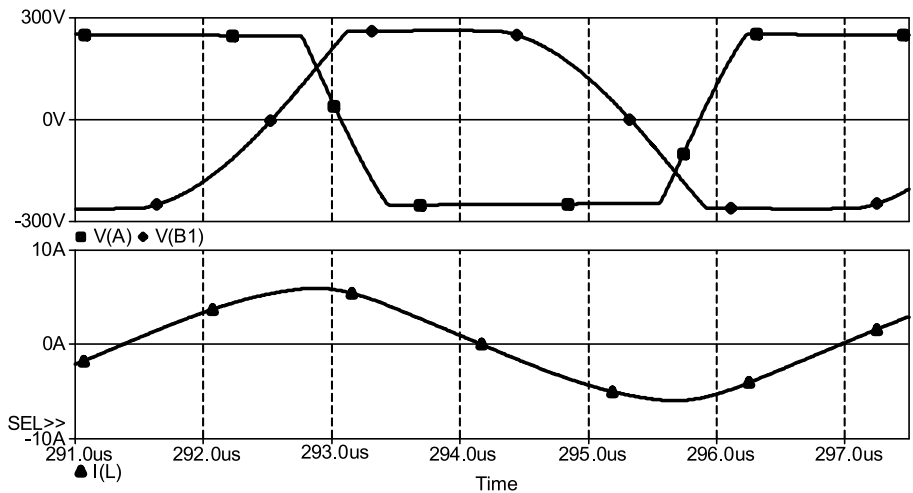


Fig. 6 – Simulation results in the main medial mode ( $R = 2.2$  and  $R_T = 23$  k $\Omega$ ).

Figs. 6 and 7 show that in the *medial* and *conterminal* modes voltage  $V(B1)$  has better amplitude compared to voltage  $V(A)$ . This confirms the conclusion that in relative units the converter output voltage  $U_0$  can be higher than the converter input voltage  $U_d$ .

The simulation results show that the snubbers and the matching transformer parameters do not significantly affect the converter's dynamic behaviour under optimal trajectory control. Fig. 8 shows the transitions from one steady state trajectory to another during step-changing of the control parameter and at  $R_T = 3$  k $\Omega$ .

The state variables are the current through the inductor  $L - I(L)$  and the voltage across the capacitor  $C - V(C)$ . In the first case (Fig. 8a) the control parameter changes from  $R_1 = 2.2$  to  $R_2 = 3.3$  at output voltage value  $U_0 = 135$  V. Fig. 8b shows the response to a change from  $R_1 = 3.3$  to  $R_2 = 2.2$  and  $U_0 = 216$  V. In both cases the converter reaches the new steady state trajectory in a minimal time interval limited only by the resonant tank circuit properties.

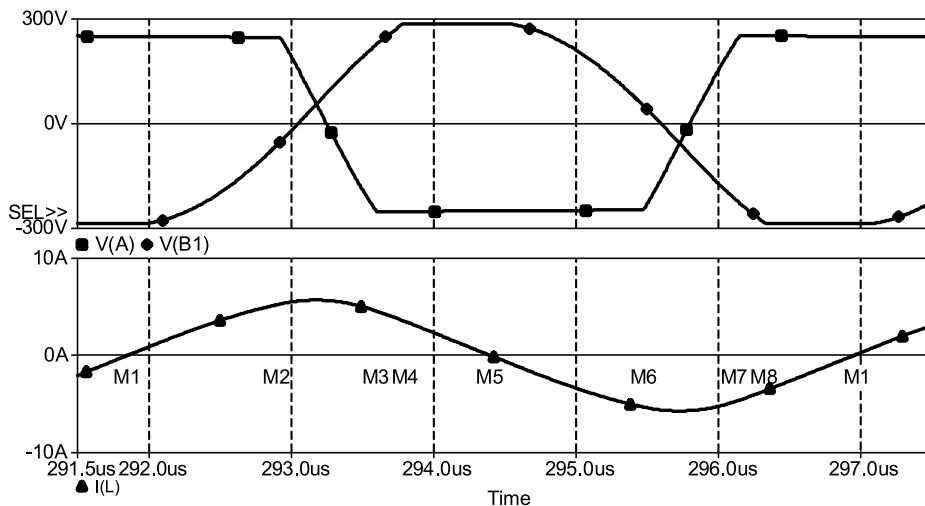


Fig. 7 – Simulation results in the conterminal operating mode ( $R = 2.2$  and  $R_0 = 70$  k $\Omega$ ).

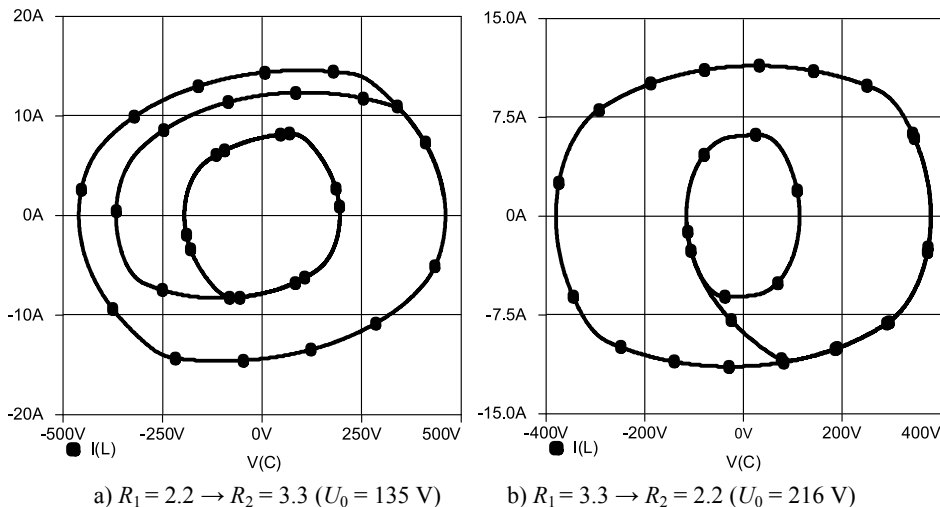
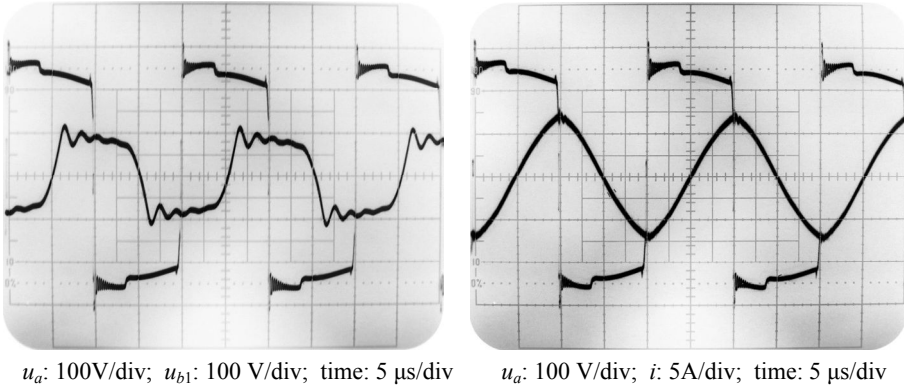


Fig. 8 – Dynamic behaviour of the converter with control parameter changes ( $R_0 = 3$  k $\Omega$ ).

The acquired theoretical results are also confirmed experimentally by a prototype built on the above design data. The following estimated values were established as parameters of the utilized matching transformer: leakage inductance  $L_S = 3.2 \mu\text{H}$  and coil self-capacitance  $C_0 = 16.7 \text{ nF}$ .

Fig. 9 shows oscillograms of the inverter output voltage  $u_a$ , the matching transformer input voltage  $u_{b1}$ , and current  $i$  running through inductor  $L$ . They are obtained during the converter operation in the main mode. Oscillograms of the same quantities during the converter operation in *conterminal* mode are shown in Fig. 10.



**Fig. 9** – Experimental results in the main mode.

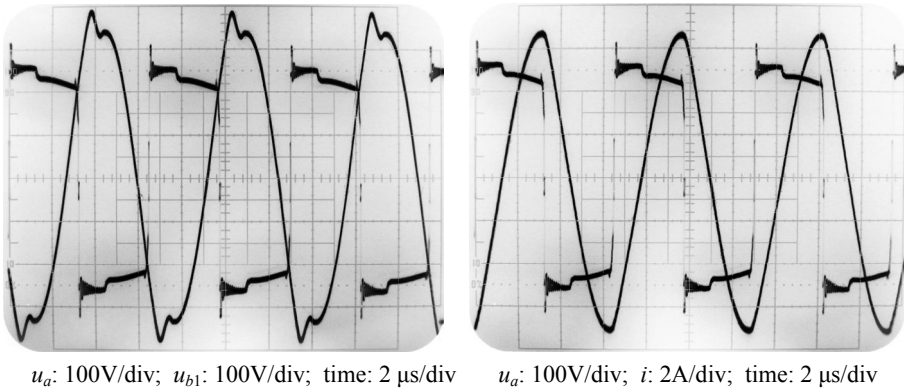


**Fig. 10** – Experimental results in the conterminal mode.

## 6 Conclusion

The operation process of a series-resonant DC/DC converter operating at frequencies higher than the resonant frequency has been analysed, considering

the effects of the damping capacitors and the coordinate transformer. The specific converter operating modes have been examined and the conditions for the operating modes have been described. Their detailed analysis has been presented in the phase plane. The output characteristics for all operating modes under optimal trajectory control have been outlined. The boundary lines between the separate operating modes of the converter, as well as the area of natural commutation of the transistors, are shown in the output characteristics plane. Results from both computer simulation with OrCAD PSpice and the experimental prototype have been acquired, confirming the results of the analysis.

Theoretical studies indicate that the ZVS conditions can be retained at high-ohm-loads and the series-resonant DC-DC converter can remain efficient even in no-load mode. For this purpose it is necessary that the coordinate transformer self-capacity is higher than the capacity of the snubbers.

The output characteristics show that in the area of low loads, the normalized output voltage value increases over one unit, which is very typical for converters with controlled rectification. This can be explained by the similarities in the operating mechanisms of the rectifier in the analysed converter.

The results from this analysis can be used to create a precise design of both the converter and the controlling system for the output voltage.

## **7 References**

- [1] Y. Cheron, H. Foch, J. Roux: Power Transfer Control Methods in High Frequency Resonant Converters, PCI Proceedings, Munich, June 1986, pp. 92 – 103.
- [2] R. Oruganti, F.C. Lee: Resonant Power Processors: Part II – Methods of control, IEEE Transaction on Industry Applications, Vol. IA-21, No. 6, Nov. 1985, pp. 1461 – 1471.
- [3] M. Boyer, J.C. Hapiot, Y. Cheron: Commande par Trajectoire Optimale de Convertisseurs a Resonance Serie, Journal de Phisique III, Vol. 5, No. 6, June 1995, pp. 727 – 741.
- [4] L. Rossetto: A Simple Control Technique for Series Resonant Converters, IEEE Transactions on Power Electronics, Vol. 11, No. 4, July 1996, pp. 554 – 560.
- [5] V. Sendanyoye, K. Al Haddad, V. Rajagopalan: Optimal Trajectory Control Strategy for Improved Dynamic Response of Series Resonant Converter, IEEE Industry Application Society Annual Meeting, Seattle, WA, USA, 7 – 12 Oct. 1990, Vol. 2, pp. 1236 – 1242.
- [6] J. Liu, L. Sheng, J. Shi, Z. Zhang, X. He: Design of High Voltage, High Power and High Frequency in LCC Resonant Converter, 24th IEEE Applied Power Electronics Conference and Exposition, Washington, USA, 15 – 19 Feb. 2009, pp. 1034 – 1038.
- [7] S. Vukosavić, N. Popov, Ž. Despotović: Power Electronics Solution to Dust Emissions from Thermal Power Plants, Serbian Journal of Electrical Engineering, Vol. 7, No. 2, Nov. 2010, pp. 231 – 252.
- [8] R. Oruganti, F.C. Lee: Resonant Power Processors: Part I – State Plane Analysis, IEEE Transaction on Industry Applications, Vol. IA-21, No. 6, Nov. 1985, pp. 1453 – 1460.

- [9] M. Anchev, G. Maleev: Analysis of a Transistor Inverter Functioning with a Frequency Higher than that of the Resonance One, *Elektrotechnica & Elektronika*, Vol. 5, No. 6, 2000, pp.12 – 17.
- [10] M. Anchev, E. Popov, G. Maleev: Integrated Analysis of DC-DC Converters Operating above or below Resonance Frequency, *Elektrotechnica & Elektronika*, 2003, pp. 35 – 39.
- [11] N. Bankov, T. Grigorova: Load Characteristics and Control System Behavioral Modeling under Optimal Trajectory Control of Series Resonant DC/DC Converters, *Journal of Electrical Engineering*, Vol. 56, No. 9/10, 2005, pp. 258 – 264.